Modeling Josephson junctions*

D. G. McDonald, E. G. Johnson, and R. E. Harris
National Bureau of Standards, Boulder, Colorado 80302
(Received 4 August 1975)

The current-voltage characteristic of a current-biased junction is calculated using the Werthamer theory. In contrast with the voltage-biased model large zero-frequency currents exist at 0°K at all bias voltages below the energy gap and the Riedel peak is directly displayed. The effect of capacitance on the I-V curve is described and the form of the subharmonic energy-gap structure is calculated using the Mattis-Bardeen model for the superconducting electrodes.

MODELING JOSEPHSON JUNCTIONS

Interest in junction modeling stems from the desire to understand the variable nature of junctions from one sample to the next and the variability across the conventional categories of tunnel junctions, point contacts, and microbridges. Observation of the subharmonic energy-gap structure in microbridges by Gregers-Hansen *et al.*[1] suggested a greater similarity with tunnel junctions and point contacts than previously supposed. But discussion of similarities remains highly speculative when the only available microscopic model is for the voltage-biased tunnel junction[2] which, incidentally, does not display subharmonic structure. Consequently we have evaluated the Werthamer tunneling theory[2] with finite external impedances and for infinite impedance, the current-biased case. The voltage-biased model has served an important role as a standard for judging the quality of practical junctions. We will show, however, that ideal tunnel junctions (i. e., without shorts or imperfections) can have quite different I-V characteristics–characteristics resembling those of point contacts[3] and microbridges.[4]

In calculating junction current it is desirable to avoid explicit spatial dependences of the current density. Consequently the junction is assumed to be small compared with all relevant electromagnetic wavelengths and no larger than a few Josephson penetration depths[5] as well as having zero applied magnetic field. Under these conditions the current is given by Werthamer's Eq. (11) [hereafter referred to as Eq. W(11)]:

$$g(t)=\frac{\Delta}{R}\,\mathrm{Im}\int_{-\infty}^{\infty} d\omega\, d\omega' \left[M(\omega)M^*(\omega')e^{-i(\omega-\omega')t} \times j_1(\omega'+\tfrac{1}{2}\omega_0)+M(\omega)M(\omega')e^{-i(\omega+\omega'+\omega_0)t}j_2(\omega'+\tfrac{1}{2}\omega_0)\right], \tag{1}$$

where Werthamer's $W(\omega)$ has been replaced by $\exp(-\frac{1}{2}i\alpha)\,M(\omega)$. The only other change from Werthamer's notation is that we have factored Δ/R, with units of amperes, from j_1 and j_2.

To formulate the problem for digital computation $M(\omega)$ is expanded harmonically about the self-oscillation frequency ω_0:

$$M(\omega)\equiv\sum_{j=-\infty}^{\infty} M_j\delta(\omega+j\omega_0), \tag{2}$$

where the M_j are complex numbers. Combining Eqs. (1) and (2) gives, after suitable shifting of indices

$$g(t)=\frac{\Delta}{R}\left(I_0+\mathrm{Re}\sum_{n=1}^{\infty}(I_{1n}+I_{2n})e^{-in\omega_0 t}\right). \tag{3}$$

The dimensionless complex harmonic current amplitudes I_{1n} and I_{2n} are functions of j_1 and j_2, respectively. Harris's sign convention[6] is used for the j's. The detailed form of the zero-frequency current equation is

$$I_0=\sum_{k=-\infty}^{\infty}\{M_kM_k^*\,\mathrm{Im}j_1[(-k+\tfrac{1}{2})\omega_0/\omega_g] + \mathrm{Im}(M_{k+1}M_{-k})\,\mathrm{Re}j_2[(k+\tfrac{1}{2})\omega_0/\omega_g]\}, \tag{4}$$

where ω_g is the energy-gap frequency given by $2e\Delta/\hbar$.

By definition for the current-biased junction, the total current must be zero for all $n>0$:

$$I_{1n}+I_{2n}=0, \quad 0<n\leq N. \tag{5}$$

If the harmonic expansion of Eq. (2) is truncated at $j=\pm N$, then $2N+1$ M_j's must be determined and, consequently, $4N+2$ equations are required for a solution. Equations (5) number $2N$ in all.[7] An additional $2N+1$ equations are obtained from the fact that $M(\omega)$ is the Fourier transform of an exponential function [Eq. W(10)] and normalization of $M(\omega)$ requires $e^{ix}e^{-ix}=1$. Setting the absolute phase by the requirement $\mathrm{Im}M_0=0$ gives the last required equation.

Numerical solutions are obtained by specifying ω_0 (i. e., in effect the average junction voltage), guessing a set of M_j, and computing a first-derivative correction matrix which provides the

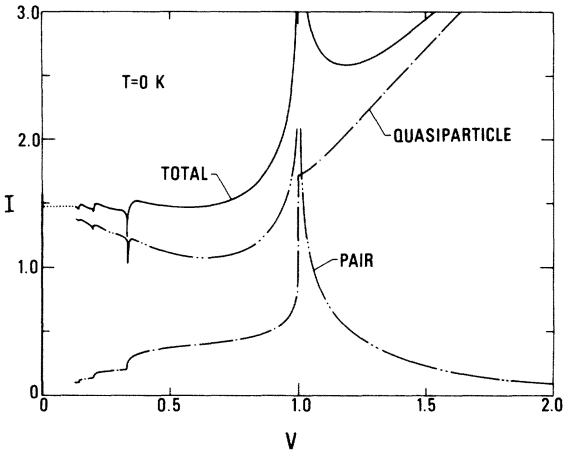

FIG. 1. Calculated I-V characteristic for a small current-biased tunnel junction. The Riedel peak occurs at a voltage of unity, and the odd subharmonic series are present at voltages of $\frac{1}{3}$, $\frac{1}{5}$, and $\frac{1}{7}$. The curve labeled total is the sum of the quasiparticle [$\mathrm{Im} j_1(\omega)$] and pair [$\mathrm{Re} j_2(\omega)$] contributions, as required by Eq. (4). To obtain practical dimensions multiply I by Δ/R and V by 2Δ where Δ is in volts and R is in ohms.

basis for a systematic iterative approach to a solution. The converged set of M_j are then substituted into Eq. (4) to obtain the zero-frequency current which is displayed in Fig. 1. This solution has been checked using an independent time domain formulation of the problem.

In sharp contrast with the voltage-biased case there are large currents at voltages below the energy gap. In this regard our model resembles Stewart's low-frequency current-biased model[8] and the experimental curves from point contacts[3] and microbridges.[4] *It also illustrates how the voltage-biased model is not fundamental to tunneling theory but is only one case of the theory.* Since it is well known from the Stewart model that current-biased junctions generate harmonics of ω_0, it is expected that a quasiparticle current would be produced at voltages well below the gap by photon assisted tunneling[9] and that is observed in Fig. 1. However it turns out that the major current below the gap is not quasiparticles, but pairs.

Before discussing the Riedel peak and related singularities of Fig. 1, let us focus on the observability of large currents below the energy gap. In Fig. 2 we illustrate the effect of shunt capacitance added to the model. As the capacitance is increased, generally the level of current below the energy gap moves continuously downward. Perhaps the most interesting aspect of this is that for a value of RC/τ_g as small as unity, the I-V curve has essentially reached the voltage biased case, i.e., very little current below the energy gap. To our knowledge the smallest value of RC/τ_g in the literature for the common form of tunneling barrier (metal oxide) is ≈ 0.5.[10] For our purposes a more interesting case is Huang and Van Duzer's[11] novel single-crystal Si barrier for which we estimate $RC/\tau_g \approx 0.1$. As expected from the present theory, the experimental I-V curve for this small value of RC/τ_g exhibits large currents below the energy gap; it resembles the curves for "catwhisker" point contacts.[3] Unfortunately the transverse dimensions of the junctions in both of the above examples are too large to avoid electromagnetic standing waves, which are not included in our theory. Consequently detailed agreement with the theory is not expected.

Returning to Fig. 1, we see the Riedel peak directly displayed in the pair current and the total current at a voltage of unity. Singularities are also present at subharmonics of the energy-gap voltage $1/m$, where m is an odd integer, but are not present for even m. This behavior is understood by observing that the response func-

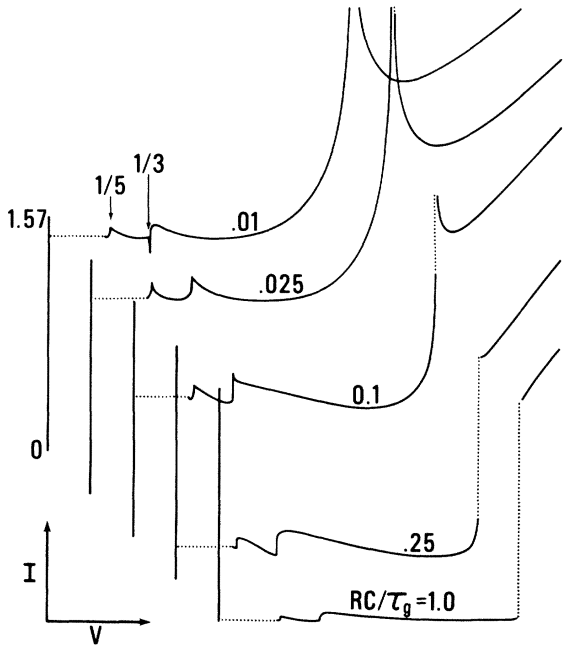

FIG. 2. Effect of shunt capacitance C on the I-V curve. R is the junction normal state resistance and τ_g is $h/2e\Delta$. Each curve is plotted with a displaced origin for clarity and with the zero-voltage current going vertically from zero to 1.57 in all cases. As the curves approach zero voltage from the right, an increasing number of harmonics are required and consequently the calculations cannot be continued to zero voltage. Dotted lines are used to visually connect the curves to their corresponding zero-voltage current and to visually relate the curves near the Riedel peak voltage of unity, when appropriate.

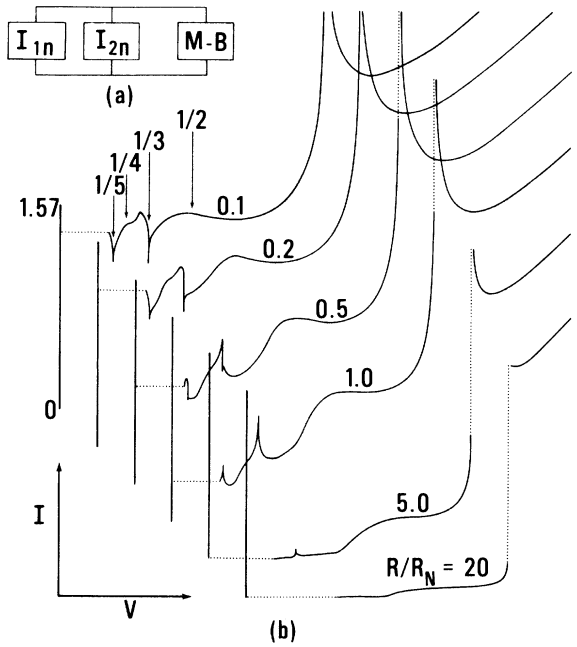

FIG. 3. (a) Junction circuit model for the nth harmonic including a Mattis-Bardeen (M-B) superconducting load. The dc circuit requires the addition of a current source and the deletion of the M-B load. (b) Calculated I-V characteristics for a small area junction as a function of R/R_N. Each curve is plotted with a displaced origin and with dotted continuations as in Fig. 2. Structure is apparent at both the even and odd subharmonics down to a voltage of $\frac{1}{5}$.

tion $\mathrm{Re}j_2(\omega)$ is singular as $\omega \to \pm 1$. Equation (4) then implies that the current is singular when $(k+\frac{1}{2})\omega_0/\omega_g = \pm 1$, a condition which produces the odd series but not an even series. Werthamer and others[12] have speculated that the even series would be produced by interaction of the junction electromagnetic fields with the superconducting electrodes, but the argument has never been given quantitative form. That can now be done with the present model. The junction is thought of as having an oscillatory component arising from j_2 terms and a shunting path represented by j_1 terms. Bulk superconductor, represented by the Mattis-Bardeen theory,[13] is added to the circuit in series with the oscillator and in parallel with the existing shunt. The circuit is shown in Fig. 3(a). For these calculations Eqs. (5) are replaced by the following:

$$I_{1n} + I_{2n} + 2(R/R_N)(\sigma/\sigma_N)_n v_n = 0, \quad 0 < n \leq N \qquad (6)$$

where $(\sigma/\sigma_N)_n$ is the Mattis-Bardeen conductivity at the nth harmonic and v_n is the corresponding dimensionless complex voltage normalized to 2Δ. The voltage is an explicit function of M_j. The normal-state resistance of the Mattis-Bardeen superconductor and the junction are R_N and R.

Numerical solutions to Eqs. (6) are displayed in Fig. 3(b) for several values of R/R_N. As R/R_N ranges from zero to large values, the solutions evolve from the current biased to the voltage biased case. As anticipated the presence of the Mattis-Bardeen superconductor does produce additional structure in the curves, most notably a broad rise in conductance near a voltage of $\frac{1}{2}$. At large values of R/R_N this structure resembles that first reported by Taylor and Burstein[14] and interpreted[12] as multiparticle tunneling. Another school of thought[12] favors a Josephson-effect explanation. These calculations support the latter position, particularly the curves for $R/R_N = 5$ and 20. Quantitative comparison with experiment is not possible at this time since the experiments include spatial effects which are ignored here. Furthermore capacitance is not included in the circuit with the M-B load because it introduces additional structure which is beyond the scope of this discussion. In practical experiments noise effects will determine the actual transition point for crossing subharmonic singularities and the extent of the observed hysteresis due to the negative resistance regions.

A small broad peak at a voltage of $\frac{1}{4}$ is also apparent in the curves for $R/R_N = 0.1$ to 1.0. Since the structure at $\frac{1}{2}$ and $\frac{1}{4}$ has quite a different appearance than the odd series, there is a tendency to be unsatisfied with this explanation of the experiments. Qualitative agreement between theory and experiment might be achieved by including mechanisms for rounding the Riedel singularity (recently discussed by Hasselberg[15]) or considering spatial or more detailed circuit effects.

We want to acknowledge the expert programming assistance of Bernice Bender and useful discussions with R. L. Peterson, J. W. Wilkins, and M. Tinkham.

*Research partially supported by the Office of Naval Research.

[1]P. E. Gregers-Hansen, E. Hendricks, M. T. Levinsen, and G. R. Pickett, Phys. Rev. Lett. 31, 524 (1973).
[2]N. R. Werthamer, Phys. Rev. 147, 255 (1966).
[3]J. E. Zimmerman, Proceedings of the 1972 Applied Superconductivity Conference, IEEE Publication No. 72CH0682-5-TABSC, New York, p. 544 (unpublished).
[4]P. W. Anderson and A. H. Dayem, Phys. Rev. Lett. 13, 195 (1964).
[5]C. S. Owen and D. J. Scalapino, Phys. Rev. 164, 538 (1967).
[6]R. E. Harris, Phys. Rev. 10, 84 (1974); 11, 3329 (1975).

[7]Truncation of the M_j spectrum at $j=\pm N$ implies currents at frequencies up to the $2N+1$ harmonic. Equations (5) are applied only to the first N of these, with N being made large enough that the zero-frequency current is numerically independent of N.
[8]W. C. Stewart, Appl. Phys. Lett. 12, 277 (1968).
[9]A. H. Dayem and R. J. Martin, Phys. Rev. Lett. 8, 246 (1962).
[10]R. F. Broom, W. Jutzi, and Th. O. Mohr, IEEE Trans. Magn. MAG-11, 755 (1975).
[11]C. L. Huang and T. Van Duzer, IEEE Trans. Magn. MAG-11, 766 (1975); Appl. Phys. Lett. 25, 753 (1974).
[12]Pertinent references and discussion can be found in L. E. Hasselberg, M. T. Levinsen, and M. R. Samuelsen, Phys. Rev. B 9, 3757 (1974).
[13]D. C. Mattis and J. Bardeen, Phys. Rev. 111, 412 (1958).
[14]B. N. Taylor and E. Burstein, Phys. Rev. Lett. 10, 14 (1963).
[15]L. E. Hasselberg, J. Phys. F 4, 1433 (1974).